Niobium Bis-alkylidene Complexes Prepared by a Multi-Electron Redox Process

Uriah J. Kilgore, John Tomaszewski, Hongjun Fan, John C. Huffman, and Daniel J. Mindiola*

Department of Chemistry, Indiana University-Bloomington, 800 E. Kirkwood Avenue, Bloomington, Indiana 47405

Received August 11, 2007

High-valent niobium bis-alkylidene complexes have been structurally authenticated along with the first paramagnetic Nb(IV) alkylidene. The bis-alkylidene complexes presented in this work are thought to be generated via a redox process involving α-hydride elimination from a transient Nb(III) bis-alkyl complex. X-ray diffraction, DFT, and multinuclear NMR studies are consistent with these bis-alkylidenes having drastically different chemical environments.

Introduction

Since the development of the first niobium bis-alkylidene system by Schrock and co-workers in 1978, $(PMe_3)_2Nb(=CHCMe_3)_2(CH_2CMe_3)$,[1] the terminal niobium bis-alkylidene motif has virtually vanished from the literature and its reactivity, for the most part, remains unexplored.[1,2] This is rather surprising given that high oxidation state transition-metal alkylidenes have shown themselves to be indispensable tools for processes such as olefin metathesis,[3−7] alkyne polymerization,[8−10] Wittig-type reactions,[7,11] and more recently, alkane metathesis.[12,13] To date, crystallographically characterized examples of terminal Nb(V) bis-alkylidenes are unknown, a striking contrast to the heavier Ta(V) analogue.[14−17] The syntheses of the aforementioned metal bis-alkylidene complexes involve a protocol in which high-valent M(V) precursors are used (M = Nb or Ta). As such, limitations in preparing and isolating Nb(V) bis-alkylidene compounds might be attributed to the ability of the central metal atom to populate low-valent states, especially the +4 oxidation state. Consequently, treatment of the metal halide precursor with alkyl lithium or Grignard reagents, which are frequently employed in the construction of Ta(V) bis-alkylidenes, may be met with limited success for Nb(V) due to its inherent ability to be reduced by an incoming nucleophile.

Herein we present a reliable synthetic route to the first structurally authenticated examples of terminal Nb(V) bis-alkylidene complexes where the bis-alkylidene ligands in question are neopentylidene and trimethylsilylmethylidene. In the course of the preparation of bis-alkylidenes, the first example of a paramagnetic Nb(IV) alkylidene was isolated and structurally characterized. The latter complex was shown not to be a viable intermediate along the formation of the niobium bis-trimethylsilylmethylidene.

Results and Discussion

Given that niobium has repeatedly been shown to access oxidation states +3[18−20] and +4,[21,22] we thought it might be feasible to pursue complexes bearing niobium−carbon multiple bonds by introducing a bulky alkyl group on a low-valent metal halide precursor with reagents such as alkyl lithium, Grignard reagents, or dialkylmagnesium compounds followed by an oxidatively induced α-abstraction step.[11,23] To realize this goal, we employed the robust supporting ligand PNP ($N[2\text{-}P(CHMe_2)_2\text{-}4\text{-}Me\text{-}C_6H_3]_2^-$), as this scaffold has demonstrated the potential to stabilize titanium and zirconium complexes bearing metal−carbon multiple bonds.[24−28] In addition, this ligand framework

* To whom correspondence should be addressed. E-mail: mindiola@indiana.edu.

(1) Fellmann, J. D.; Rupprecht, G. A.; Wood, C. D.; Schrock, R. R. *J. Am. Chem. Soc.* **1978**, *100*, 5964.
(2) Fellmann, J. D.; Rupprecht, G. A.; Schrock, R. R. *J. Am. Chem. Soc.* **1979**, *101*, 5099.
(3) Schrock, R. R. *Chem. Commun.* **2005**, 2773.
(4) Schrock, R. R. *J. Mol. Catal. A* **2004**, *213*, 21.
(5) Schrock, R. R.; Hoveyda, A. H. *Angew. Chem., Int. Ed.* **2003**, *42*, 4592.
(6) Schrock, R. R. *Pure Appl. Chem.* **1994**, *66*, 1447.
(7) Schrock, R. R. *Chem. Rev.* **2002**, *102*, 145.
(8) Buchmeiser, M. R. *Chem. Rev.* **2000**, *100*, 1565.
(9) Schrock, R. R.; Luo, S.; Lee, J. C., Jr.; Zanetti, N. C.; Davis, W. M. *J. Am. Chem. Soc.* **1996**, *118*, 3883.
(10) Schlund, R.; Schrock, R. R.; Crowe, W. E. *J. Am. Chem. Soc.* **1989**, *111*, 8004.
(11) Mindiola, D. J.; Bailey, B. C.; Basuli, F. *Eur. J. Inorg. Chem.* **2006**, *2006*, 3135.
(12) Blanc, F.; Coperet, C.; Thivolle-Cazat, J.; Basset, J.-M. *Angew. Chem., Int. Ed.* **2006**, *45*, 6201.
(13) Coperet, C.; Maury, O.; Thivolle-Cazat, J.; Basset, J.-M. *Angew. Chem., Int. Ed.* **2001**, *40*, 2331.
(14) Churchill, M. R.; Youngs, W. J. *Inorg. Chem.* **1979**, *18*, 1930.
(15) Churchill, M. R.; Youngs, W. J. *J. Chem. Soc., Chem. Commun.* **1978**, 1048.
(16) Diminnie, J. B.; Hall, H. D.; Xue, Z. *Chem. Commun.* **1996**, 2383.
(17) Gerber, L. C. H.; Watson, L. A.; Parkin, S.; Weng, W.; Foxman, B. M.; Ozerov, O. V. *Organometallics* **2007**, ASAP Article.
(18) Fryzuk, M. D.; Kozak, C. M.; Bowdridge, M. R.; Jin, W.; Tung, D.; Patrick, B. O.; Rettig, S. J. *Organometallics* **2001**, *20*, 3752.
(19) Fryzuk, M. D.; Jafarpour, L.; Rettig, S. J. *Organometallics* **1999**, *18*, 4050.
(20) Roskamp, E. J.; Pedersen, S. F. *J. Am. Chem. Soc.* **1987**, *109*, 6551.
(21) Kilgore, U. J.; Yang, X.; Tomaszewski, J.; Huffman, J. C.; Mindiola, D. J. *Inorg. Chem.* **2006**, *45*, 10712.
(22) Fryzuk, M. D.; Shaver, M. P.; Patrick, B. O. *Inorg. Chim. Acta* **2003**, *350*, 293.
(23) Mindiola, D. J. *Acc. Chem. Res.* **2006**, *39*, 813.
(24) Bailey, B. C.; Fout, A. R.; Fan, H.; Tomaszewski, J.; Huffman, J. C.; Gary, J. B.; Johnson, M. J. A.; Mindiola, D. J. *J. Am. Chem. Soc.* **2007**, *129*, 2234.
(25) Bailey, B. C.; Basuli, F.; Huffman, J. C.; Mindiola, D. J. *Organometallics* **2006**, *25*, 3963.
(26) Bailey, B. C.; Fan, H.; Huffman, J. C.; Baik, M.-H.; Mindiola, D. J. *J. Am. Chem. Soc.* **2006**, *128*, 6798.
(27) Bailey, B. C.; Fan, H.; Baum, E. W.; Huffman, J. C.; Baik, M.-H.; Mindiola, D. J. *J. Am. Chem. Soc.* **2005**, *127*, 16016.

10.1021/om7008233 CCC: $37.00
Publication on Web 10/31/2007

Scheme 1. Syntheses of Complexes 2−5 from Precursor 1

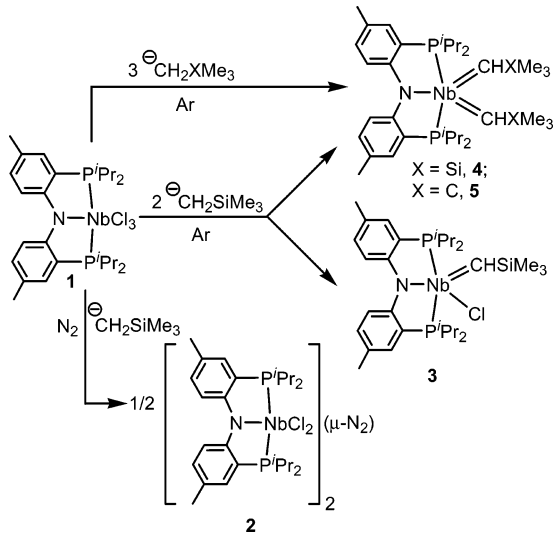

has recently been used as a ancillary support for transient Nb(III) fragments capable of activating atmospheric nitrogen as well as cleaving the N═N bond in azobenzene.[21]

Accordingly, the Nb(IV) precursor (PNP)$NbCl_3$[21] (**1**) was treated with the alkyl reagents $LiCH_2XMe_3$, $Mg(CH_2XMe_3)_2$, or the corresponding Grignard (X = Si and C). In all cases, we observed that treatment of **1** with these nucleophiles led to reduction. For example, treatment of **1** with 1 equiv of $LiCH_2SiMe_3$ under an atmosphere of dinitrogen resulted in the formation of $[(PNP)NbCl_2]_2(\mu\text{-}N_2)$ (**2**) (Scheme 1) in 26% yield, a complex that has been previously synthesized in higher yield by reduction of **1** with Bu_3SnH under an atmosphere of N_2.[21] Altering the stoichiometry under an atmosphere of N_2, e.g., using an increased amount of alkyl lithium, Grignard, or dialkylmagnesium, resulted in complicated mixtures that typically included traces of **2** (assayed by ^{1}H NMR spectra). When **1** was treated with 1 equiv of $LiCH_2SiMe_3$ under argon, a mixture of products was also observed in the ^{1}H NMR spectra. However, treatment of **1** with 2 equiv of $LiCH_2SiMe_3$ under argon resulted in formation of a paramagnetic product, namely. the alkylidene complex (PNP)Nb═$CHSiMe_3$(Cl) (**3**), along with traces of a diamagnetic material (Scheme 1). Formation of **3** can be optimized via treatment of **1** with 1 equiv of a milder alkyl reagent such as $Mg(CH_2SiMe_3)_2$ or 2 equiv of the corresponding Grignard with exceedingly slow addition times of the alkyl reagent to the niobium precursor. This result implied that using an excess above 2 equiv of alkyl reagent might improve formation of the diamagnetic side-product since complex **3** appeared to be dependent on the concentration of the magnesium alkylating reagent. Unfortunately, isolation of pure **3** has proven a difficult task since its formation of **3** is always accompanied by production of a diamagnetic product (vide infra) when such a mixture is assayed by ^{1}H NMR spectroscopy and MS-CI.

The connectivity of paramagnetic **3** was supported by single-crystal X-ray diffraction studies showing a five-coordinate alkylidene complex with a short Nb═C (1.931(2) Å) bond and a Nb═C−Si angle of 138.96(17)° (Figure 1). Clearly, the latter parameters are consistent with the assignment of a niobium−carbon double bond. The Evans magnetic moment of μ_{eff} = 1.92(4) measured in C_6D_6 solution at 25 °C is in accordance with a monomeric d^1 niobium species, while the isotropic X-band EPR spectrum recorded in toluene reveals a metal-based electron (g_{iso} = 1.967) with hyperfine coupling to ^{93}Nb (A_{iso} = 148.60 G) and superhyperfine coupling to the two ^{31}P atoms of the PNP ligand (A_{iso} = 20.26 G, Figure 1). Our EPR spectrum therefore demonstrates that complex **3** appears to be the only Nb(IV) species isolated from the reaction of **1** and the magnesium alkyl reagent.

As anticipated, we found that treatment of **1** with 3 equiv of trimethylsilylmethyl alkyl reagent (Li^+, Mg^{2+}, or $MgCl^+$ salts) under an atmosphere of argon led to an increase in the formation of the diamagnetic species, which could be isolated in pure form upon workup of the reaction mixture (Scheme 1). The product, later identified to be the bis-alkylidene species (PNP)Nb(═$CHSiMe_3)_2$ (**4**), on the basis of multinuclear NMR spectra and single-crystal X-ray diffraction studies (vide infra), was isolated in 33% yield. Analogous to the synthesis of **4**, treatment of **1** with 1.5 equiv of $Mg(CH_2CMe_3)_2$ or 3 equiv of the Grignard under an atmosphere of argon yielded the bis-neopentylidene product (PNP)Nb(═$CHCMe_3)_2$ (**5**) (Scheme 1). Surprisingly, we were unable to isolate the putative "(PNP)Nb═$CHCMe_3$(Cl)" complex when applying slow addition of 2 equiv of $^-CH_2CMe_3$ source to **1**.

Structural assignment of **4** and **5** is based on a combination of multinuclear NMR spectroscopic studies and single-crystal X-ray diffraction data. ^{31}P NMR spectra for both complexes show broad, virtually featureless signals at room temperature, but cooling the solutions to −50 °C decoalesces each broad resonance into two singlets (see Figure S1 in the Supporting Information). Unfortunately, we were unable to resolve the J_{PP} coupling for each resonance at low temperatures presumably due to coupling of ^{31}P to the quadrupolar niobium center. The ^{13}C NMR spectrum of **4** displays two broad resonances at 272.2 (J_{CH} = 120 Hz) and 249.7 (J_{CH} = 93 Hz) ppm, corresponding to the Nb═*C*− alkylidene carbons (Table 1). Likewise, ^{13}C NMR studies of complex **5** reveal similar features for the alkylidene carbons at 282.5 (J_{CH} = 101 Hz) and 237.1 (J_{CH} = 80 Hz) ppm (Table 1). The room-temperature ^{29}Si NMR spectrum of **4** consists of two singlets centered at −15.4 and −18.2 ppm, further substantiating the assertion that two trimethylsilylmethylidene environments are present. In addition, the ^{1}H NMR spectra of **4** and **5** were also consistent with two distinctly different alkylidene environments. Conducting 2-D NMR experiments on **4** (gHMQC) clearly expose correlations of the α-hydrogens at 12.17 and 7.52 ppm to the alkylidene carbons found at 272.2 and 249.7 ppm, respectively (Figure S2 in the Supporting Information).[29] The same experiments carried out on complex **5** correlate the alkylidene ^{1}H NMR resonances at 10.97 and 2.2 ppm to the alkylidene α-carbons 282.5 (J_{CH} = 101 Hz) and 237.1 ppm (J_{CH} = 80 Hz), respectively (Figure S3 in the Supporting Information).[30] Furthermore, the J_{CH} values we observe suggest that both **4** and **5** may be experiencing α-hydrogen agostic interactions (Table 1).

Schrock and co-workers observed similar behavior in the case of tantalum bis-alkylidenes and reported the two different

(28) Weng, W.; Yang, L.; Foxman, B. M.; Ozerov, O. V. *Organometallics* **2004**, *23*, 4700.

(29) Acquisition parameters for **4**: Varian INOVA 500 MHz gHMQC, number of scans = 128, recycle delay = 1.5 s, ^{1}H sweep width = 8000 Hz, ^{13}C sweep width = 40221.2 Hz, acquisition time = 0.193 s, one-bond coupling = 140 Hz. The gHMQC used a broadband inversion pulse on C13, which was a 323.7 μs composite adiabatic WURST2 pulse covering ca. 50 kHz. The pulse was generated using Pbox in VNMR based on a reference pulse width of 13.89 μs at a transmitter power of 59 dB.

(30) Acquisition parameters for **5**: Varian INOVA 500MHz gHMQC, number of scans = 16, recycle delay = 1.5 s, ^{1}H sweep width = 8000 Hz, ^{13}C sweep width = 40221.2 Hz, acquisition time = 0.193 s, one-bond coupling = 100 Hz. The gHMQC used a broadband inversion pulse on C13, which was a 323.7 μs composite adiabatic WURST2 pulse covering ca. 50 kHz. The pulse was generated using Pbox in VNMR based on a reference pulse width of 13.89 μs at a transmitter power of 59 dB.

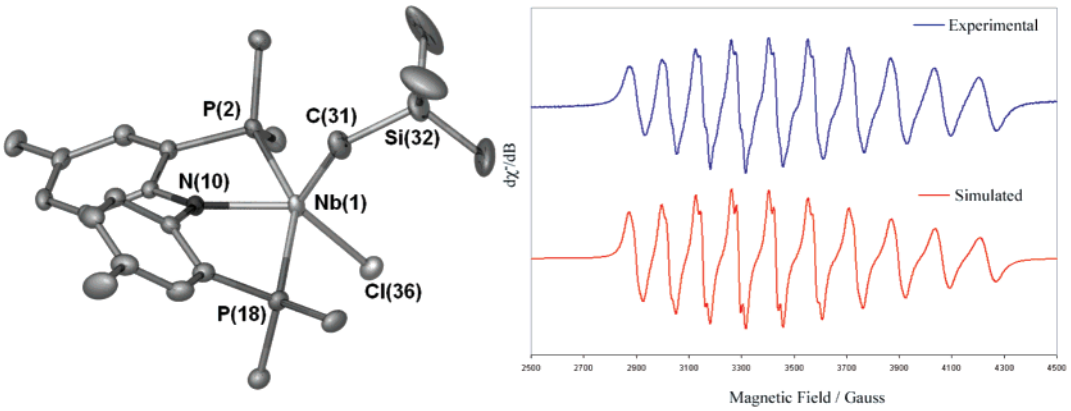

Figure 1. Molecular structure of complex **3** (left) with thermal ellipsoids at the 50% probability level and with H atoms and ^{i}Pr methyls groups omitted for clarity (left). Selected bond lengths (angstroms) and angles (degrees): Nb(1)−C(31), 1.931(2); Nb(1)−Cl(36), 2.4378-(7); Nb(1)−N(10), 2.122(6); Nb(1)−P(2), 2.5859(6); Nb(1)−P(18), 2.5744(7); C(31)−Nb(1)−Cl(36), 112.76(9); Si(32)−C(31)−Nb(1), 138.96(17). The right figure displays the X-band EPR spectrum of **3** recorded at room temperature in toluene (715 μM solution). Acquisition parameters: frequency = 9.86 GHz, MF = 100 kHz, MA = 10 G, P = 0.2011 mW.

Table 1. Experimental and Computed NMR Chemical Shifts for α-Carbons and α-Hydrogens of 4 and 5

complex	exptl ^{13}C NMR: δ α-C [J_{CH} (Hz)]	calcd ^{13}C NMR: δ α-C	exptl ^{1}H NMR δ α-H	calcd ^{1}H NMR δ α-H
4	272.2 [120], 249.7 [93]	284.9, 260.5	12.17, 7.52	13.90, 11.20
5	282.5 [101], 237.1 [80]	302.0, 248.5	10.97, 2.20[a]	12.8, 6.00

[a] Signal located and assigned by gHMQC.

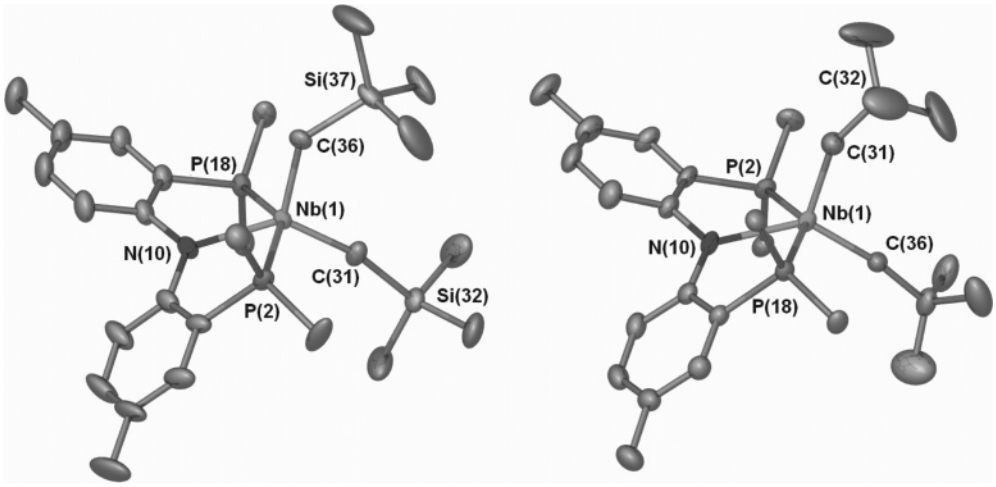

Figure 2. Molecular structure of complexes **4** (left) and **5** (right) with thermal ellipsoids at the 50% probability level and H and ^{i}Pr methyl groups omitted for clarity. Selected bond lengths (Å) and angles (deg) for **4**: Nb(1)−C(31), 1.8651(19); Nb(1)−C(36), 1.999(2); Nb(1)−N(10), 2.1745(11); Nb(1)−P(2), 2.5836(4); Nb(1)−P(18), 2.584674); Nb(1)−C(31)−Si(32), 168.25(13); Nb(1)−C(36)−Si(37), 144.70-(11); P(2)−Nb(1)−P(18), 147.320(13); for **5**: Nb(1)−C(31), 1.976(8); Nb(1)−C(36), 1.891(6); Nb(1)−N(10), 2.201(3); Nb(1)−P(18), 2.5753(13); Nb(1)−P(2), 2.5960(14); Nb(1)−C(31)−C(32), 153.8(8); Nb(1)−C(36)−C(37), 170.8(7); P(18)−Nb(1)−P(2), 147.23(4).

alkylidene resonances to equilibrate with a $\Delta G^{\ddagger}$ ranging from 13 kcal/mol (300 K) to 17 kcal/mol (373 K) for the more hindered environment.[1] In our case, variable-temperature NMR studies do in fact disclose equilibration of the $SiMe_3$ or CMe_3 alkylidene groups for **4** and **5**, respectively (see Figure S4 in the Supporting Information). At room temperature in C_6D_6, the ^{t}Bu methyl protons of complex **5** coalesce at 1.43 ppm. In contrast, the room-temperature ^{1}H NMR spectrum of **4** reveals two $SiMe_3$ singlets at 0.48 and 0.25 ppm, and the system must be heated to 60 °C before coalescence of the $SiMe_3$ resonances occurs. Consequently, the bis-alkylidenes reported here equilibrate with $\Delta G^{\ddagger}_{298} \approx 15$ kcal/mol for complex **5** and $\Delta G^{\ddagger}_{333} \approx 16$ kcal/mol in the case of complex **4**. Such coalescence could be a result of rotation about the Nb−C bonds. In addition, room-temperature ^{31}P NMR spectra for **4** do in fact suggest that the phosphorus groups on PNP become equivalent. A rapid dissociation/association of one of the phosphine pendant donor arms might be responsible for this equivalence; alternatively, this occurrence could be due to rapid rotation of the alkylidene ligands (see Experimental Section and Supporting Information).

X-ray diffraction studies further substantiate our claims for bis-alkylidene formation in **4** and **5** (Figure 2). Each molecule takes on pseudo-trigonal bipyramidal geometries with two alkylidene ligands and a PNP amide nitrogen in the equatorial plane. The meridional constraint imposed by the PNP pincer scaffold forces the two alkylidene ligands to a cis orientation.

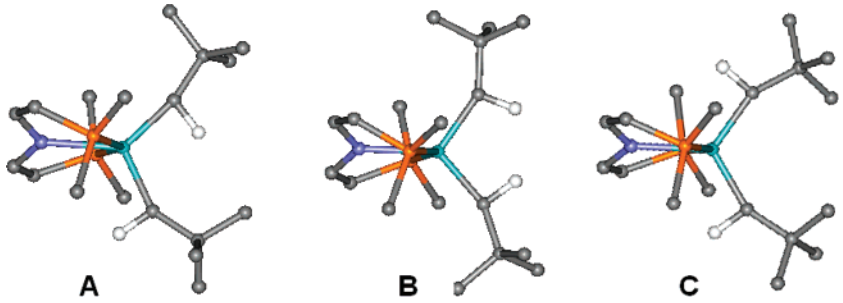

Figure 3. Possible isomeric structures for complexes **4** and **5** looking down the P−Nb−P axis. Only the isomers for complex **5** are shown for the purpose of clarity. The PNP aryl backbone and ^{i}Pr methyls have been omitted for clarity.

Notably, the direction of the XMe_3 groups (X = Si or C) suggests substantial distortion of the alkylidene ligand from an idealized sp^2-hybridized geometry (Figure 2); specifically, each alkylidene ligand is distorted to a different extent (i.e., one alikylidene ligand appears to be more linear than another). Due to crystallographic disorder in the Nb=CHXMe$_3$ ligands of **4** and **5**, it is difficult to ascertain the precise location of the alpha-alkylidene carbon protons. On the basis of this limitation, one could propose three probable orientations (forms **A**−**C**, Figure 3) for the alkylidene ligands. DFT analysis of compounds **4** and **5** suggests that the ground state geometry for either system is isomer **A**, where the orientation of one alkylidene hydrogen points into the C=Nb=C groove, while the other proton points out of the pocket in an overall propeller-like fashion. Furthermore, our calculated ^{13}C NMR chemical shifts for isomers **A**−**C** in **4** and **5** reveal that the model that we propose, isomer **A**, best agrees with the observed chemical shifts for the two alkylidene α-carbons (Table 1). Although our calculated ^{1}H NMR chemical shifts for the alkylidene α-hydrogens are ambiguous (Table 1), they do support the assertion that these protons are experiencing difference chemical environments (especially in the case of **5**).

Although formation of **3** probably involves generation of a Nb(IV) bis-alkyl chloride species, (PNP)Nb(CH_2SiMe_3)$_2$(Cl), which then undergoes α-hydrogen abstraction, its formation might be competitive with that of **4**. Conversely, the syntheses of the bis-alkylidene products **4** and **5** using 3 equiv of alkyl source seem dubious unless a redox process is invoked. Indeed, Hoffman and co-workers have observed a similar phenomenon where a Nb(V) bis-imide species was formed when the Nb(IV) starting material, $NbCl_4(PMe_3)_2$, was treated with two or more equivalents of LiNH(2,6-^{i}Pr$_2$C$_6$H$_3$).[31] However, no mention of a reaction pathway to the bis-imide product was discussed in their work. The ability of the alkyl reagent to convert **1** to **2** (vide supra) suggests that one of the three equivalents of alkyl reagent has been used as a sacrificial reductant. As a result, we propose that complexes **4** and **5** are formed via a putative (PNP)-Nb(CH_2XMe_3)$_2$ (**W**) species (Scheme 2), which subsequently undergoes α-hydride elimination to produce the alkylidene-alkyl hydride (PNP)Nb=CHXMe$_3$(H)(CH_2XMe_3) (**Y**). By means of H_2 elimination, intermediate **Y** could convert to the bis-alkylidene **4** or **5** in a concerted manner. However, H_2 elimination in **Y** could also result in formation of the alkylidyne-alkyl (PNP)Nb≡CXMe$_3$(CH_2XMe_3) (**Z**), which would then undergo α-hydrogen migration to furnish the bis-alkylidene framework (Scheme 2). The latter pathway is not unreasonable to propose since Schrock and co-workers have observed the conversion of tantalum(V) alkylidyne-alkyl to the bis-alkylidene.[1] In fact, DFT analysis for the computed structure of

Scheme 2. Proposed Mechanism for Formation of Complexes 4 and 5

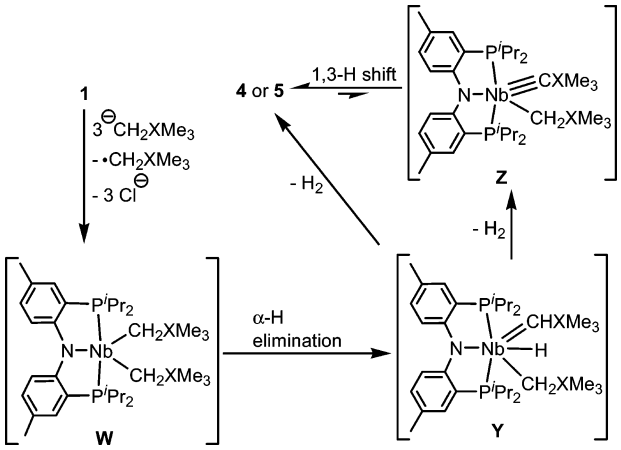

intermediate **Z** (for both $SiMe_3$ and CMe_3 analogues) suggests such a species to lie considerably higher in energy (13 and 12 kcal/mol, respectively) than the bis-alkylidene tautomers **4** and **5**.[32] However, the barrier to interconversion must be substantial, since we have been unable to observe any NMR spectroscopic evidence suggesting formation of a putative **Z** species at higher temperatures (25−90 °C).

Unfortunately, attempts to confirm the evolution of H_2 by ^{1}H NMR spectra have been inconclusive, but given the complicated nature of these reactions (e.g., low yield, other metal-based products), we propose that another species present in solution could be consuming H_2 (e.g., compound **3** or a putative Nb(III) species) to form as yet unidentified products. Given the multiple steps as well as multielectron redox processes likely involved in the formation of compounds such as **4** and **5**, we cannot eliminate the possibility of other competing side reactions or intermolecular redox processes being responsible for the formation of these bis-alkylidene complexes. We do, however, have compelling evidence to suggest that **3** is not likely an intermediate along the formation of the bis-alkylidenes inasmuch as treatment of such (contaminated with traces of **4**) with a $^{-}$CH$_2$SiMe$_3$ reagent did not result in any detectable increase in the concentration of diamagnetic **4** when the mixture was assayed by ^{1}H NMR spectroscopy using an internal standard (see Experimental Section for details). Likewise, we believe that the presence of N_2 interferes with formation of **4** and **5**, since treatment of **2** with various alkyl reagents (one or more equivalents) results in formation of a myriad of products, none of which correspond to **4** or **5** when the reaction mixture is assayed by ^{1}H NMR spectroscopy. As a result, **2** cannot be an intermediate to the bis-alkylidene complexes presented in this work.

(31) Bott, S. G.; Hoffman, D. M.; Rangarajan, S. P. *Inorg. Chem.* **1995**, *34*, 4305.

(32) See Supporting Information for details.

The successful syntheses and structural characterization of these niobium bis-alkylidenes should allow us to thoroughly study their reactivity. Preliminary reaction chemistry, however, suggests complexes such as **4** to be exceedingly robust given their failure to react with substrates such as ethene, imines, azobenzene, benzophenone, and diphenylacetylene. We are currently exploring the reactivity of **5**, although we expect such a scaffold to be equally robust to that of **4**.

Conclusions

In summary, we have synthesized and structurally characterized the first paramagnetic niobium (IV) alkylidene, as well as thoroughly characterized two niobium bis-alkylidene complexes. We speculate that these bis-alkylidene complexes are formed via a multielectron process stemming from a one-electron reduction of Nb(IV), followed by α-hydrogen and H_2 elimination steps. Although we have evidence to indicate that the paramagnetic Nb(IV) mono-alkylidene species **3** or complex **2** are not generated as an intermediate along the formation of **4** or **5**, we have no compelling evidence to support our proposed mechanism depicted in Scheme 2. Despite this, our approach to the generation of niobium bis-alkylidene frameworks appears to be a reliable method to incorporate this rare type of functionality and must represent a redox process involving multiple electrons. The bis-alkylidene complexes we have reported in this work appear to contain two unique alkylidene environments, which equilibrate upon heating. However, these systems are very robust, which could be the result of the steric protection imposed by the sterically encumbering PNP framework. We are currently exploring reactions to assemble the terminal niobium alkylidyne functionality since this rare and reactive motif appears to be a possible intermediate along formation of the bis-alkylidenes reported here.

Experimental Section

General Considerations. Unless otherwise stated, all operations were performed in a M. Braun Lab Master double-dry box under an atmosphere of purified nitrogen or using high-vacuum standard Schlenk techniques under an argon atmosphere. Anhydrous solvents were dried according to literature procedures.[33] Deuterobenzene was purchased from Cambridge Isotope Laboratory (CIL), degassed, and vacuum transferred to 4 Å molecular sieves. Celite, alumina, and 4 Å molecular sieves were activated under vacuum overnight at 200 °C. Complex **1** was prepared according to the literature.[21] $ClMgCH_2CMe_3$ was purchased from Rieke Metals. $Mg(CH_2SiMe_3)_2$ and $Mg(CH_2CMe_3)_2$(dioxane) were prepared according to the literature methods.[34,35] $LiCH_2SiMe_3$ was purchased from Aldrich as a 1.0 M solution in pentane. The solution was concentrated under reduced pressure, then crystallized by storing at −35 °C. The white solid was collected, dried under reduced pressure, and stored at −35 °C. All other chemicals were used as received. CHN analyses were performed by Midwest Microlabs, Indianapolis, IN. ^{1}H, ^{13}C, ^{29}Si and ^{31}P NMR spectra were recorded on Varian 500, 400, or 300 MHz NMR spectrometers. ^{1}H and ^{13}C NMR are reported with reference to residual solvent resonances. ^{31}P NMR chemical shifts are reported with respect to external H_3PO_4 (0.0 ppm). ^{29}Si NMR shifts are reported with respect to external $SiMe_4$ at 0 ppm. Magnetic moments were obtained by the method of Evans.[36,37]

Synthesis of $[(PNP)NbCl_2]_2(\mu\text{-}N_2)$ (2) via Treatment of 1 with $LiCH_2SiMe_3$. Under an atmosphere of N_2, to a stirring solution of **1** (100 mg, 0.159 mmol) in toluene (15 mL) at −35 °C was slowly added 1 equiv of $LiCH_2SiMe_3$ (15 mg, 0.159 mmol) in toluene. The solution slowly turned from purple to a red-maroon color. The solution was allowed to stir overnight at room temperature. The volatiles were removed in vacuo, and the residue was washed with hexane and dried. The remaining solid was dissolved in diethyl ether and filtered. Crystals of complex **2** were grown from the concentrated diethyl ether solution at room temperature. Yield: 26%, yield 50 mg, 0.041 mmol.

Synthesis of (PNP)Nb═CHSiMe$_3$(Cl) (3). Under an atmosphere of argon, to a toluene solution (30 mL) of $(PNP)NbCl_3$ (**1**) (200 mg, 0.318 mmol) held at 0 °C over the course of 2 h was added $ClMg(CH_2SiMe_3)$ (0.63 mmol) dissolved in benzene (2 equiv of $LiCH_2SiMe_3$ can alternatively be used). The purple solution rapidly took on a red-brown color. After stirring for 3 h, the solvent was removed in vacuo. The remaining solid was taken up into ether and filtered through a plug of Celite. The product mixture is found by ^{1}H and ^{31}P NMR spectroscopy and MS-CI to contain complex **4** as an impurity in approximately 25−30%. The filtrate was concentrated; crystals were grown from this solution at room temperature. Crystals suitable for X-ray diffraction were grown by concentrating a hexane solution and storing it for several days at room temperature. Yield: 20%, 41 mg, 0.064 mmol. MS-CI: $[M^+]$ theory 642.1935; $[M^+]$ experimental 642.1940. Magnetic moment, Evans' method: $\mu_{eff} = 1.92(4)$. X-Band EPR: [^{93}Nb] $A_{iso} = 149.2$ G; ^{31}P ($A_{iso} = 20.26$ G, Figure 1) ($g_{iso} = 1.967$).

Synthesis of (PNP)Nb(═CHSiMe$_3$)$_2$ (4). To a room-temperature solution (toluene, 10 mL) of 3 equiv of $LiCH_2SiMe_3$ (90 mg, 0.956 mmol) was slowly added **1** (200 mg, 0.318 mmol) dissolved in toluene (5 mL). The color of the solution rapidly became brown. After stirring overnight, the solution was stripped of all volatiles in vacuo. The resulting yellow-brown solid was taken up into diethyl ether, filtered through a plug of Celite, and then concentrated under reduced pressure. X-ray diffraction quality crystals were grown from the diethyl ether solution at room temperature. Analytically pure crystals may be grown by storing a concentrated pentane solution of **4** at −36 °C for several days. Yield: 33%, 73 mg, 0.105 mmol. Anal. Calcd for $C_{34}H_{60}NP_2NbSi_2$: C, 58.85; H, 8.72; N, 2.02. Found: C, 58.79; H, 8.64; N, 2.05. MS-CI: $[M^+]$ theory 693.2798, experimental 693.2800. ^{1}H NMR (25 °C, C_6D_6): δ 12.17 (s, 1H, ═C*H*SiMe$_3$), 7.53 (s, 1H, ═C*H*SiMe$_3$), 7.32 (m, 2H, Ar*H*), 6.69 (m, 4H, Ar*H*), 2.13 (s, 3H, ArC*H*$_3$), 2.09 (s, 3H, ArC*H*$_3$), 2.0 (m, 2H, C*H*Me$_2$) (obscured by $ArCH_3$ resonance), 1.9 (m, 2H, C*H*Me$_2$), 1.274, (doublet of doublets, 6H, CH*Me$_2$*), 1.143 (doublet of doublets, 12H, CH*Me$_2$*), 0.960 (m, 6H, 0.483 CH*Me$_2$*), (s, 9H, SiMe$_3$), 0.254 (s, 9H, SiMe$_3$). ^{1}H NMR (−45 °C, C_7D_8): δ 12.17 (s, 1H, ═C*H*SiMe$_3$), 7.34 (s, 1H, ═C*H*SiMe$_3$), 7.21 (m, 1H, Ar*H*), 7.16 (m, 1H, Ar*H*), 6.75 (m, 2H, Ar*H*), 6.64 (m, 2H, Ar*H*), 2.11 (s, 3H, ArC*H*$_3$), 2.05 (m, 2H, C*H*Me$_2$), 2.03 (s, 3H, ArC*H*$_3$), 1.89 (m, 2H, C*H*Me$_2$), 1.20, (m, 6H, CH*Me$_2$*), 0.964 (m, 12H, CH*Me$_2$*), 0.80 (m, 6H, 0.483 CH*Me$_2$*), 0.48 (s, 9H, SiMe$_3$), 0.24 (s, 9H, SiMe$_3$). ^{31}P NMR (25 °C, 121.5 MHz, C_6D_6): δ 52.5 (broad). ^{31}P NMR (−60 °C, 121.5 MHz, C_7D_8): δ 54.7, 51.5. ^{13}C NMR (−25 °C, 125.69 MHz, C_7D_8): δ 272.8 (Nb═*C*SiMe$_3$, J_{CH} = 120 Hz), 250.8 (Nb═*C*SiMe$_3$, J_{CH} = 93 Hz), 160.8 (*Ar*), 160.7 (*Ar*), 133.1 (*Ar*), 132.9 (*Ar*), 132.4 (*Ar*), 131.9 (*Ar*), 126.7 (*Ar*), 126.2 (*Ar*), 118.7 (*Ar*), 118.5 (*Ar*), 118.1 (*Ar*), 117.8 (*Ar*), 33.9 (Ar*Me*), 32.8 (Ar*Me*), 27.5 (d, *C*HMe$_2$), 26.6 (d, *C*HMe$_2$), 20.6 (CH*Me$_2$*or *C*HMe$_2$), 20.3 (CH*Me$_2$* or *C*HMe$_2$), 19.9 (CH*Me$_2$* or *C*HMe$_2$), 19.2 (CH*Me$_2$* or *C*HMe$_2$), 19.1 (CH*Me$_2$* or *C*HMe$_2$), 18.1 (CH*Me$_2$* or *C*HMe$_2$), 18.2 (CH*Me$_2$* or *C*HMe$_2$), 16.9 (CH*Me$_2$* or *C*HMe$_2$), 16.6 (CH*Me$_2$*), 16.0 (CH*Me$_2$*), 3.3 (Si*Me*$_3$), 2.9 (Si*Me*$_3$). ^{29}Si NMR (25 °C, 99.29 MHz, C_6D_6): δ −15.45 ($\Delta\nu_{1/2}$ = 16.9 Hz), −18.18 ($\Delta\nu_{1/2}$ = 29.6 Hz).

(33) Pangborn, A. B.; Giardello, M. A.; Grubbs, R. H.; Rosen, R. K.; Timmers, F. J. *Organometallics* **1996**, *15*, 1518.
(34) Tang, H.; Richey, H. G. *Organometallics* **2001**, *20*, 1569.
(35) Schrock, R. R.; Fellmann, J. D. *J. Am. Chem. Soc.* **1978**, *100*, 3359.
(36) Sur, S. K. *J. Magn. Reson.* **1989**, *82*, 169.
(37) Evans, D. F. *J. Chem. Soc.* **1959**, 2003.

Synthesis of (PNP)Nb(=CHCMe$_3$)$_2$ (5). Under an atmosphere of argon, a vial charged with a stir bar and (PNP)NbCl$_3$ (**1**) (200 mg, 0.318 mmol) dissolved in 10 mL of toluene was cooled to −35 °C. Over the course of 20 min was added a solution of 3 equiv of ClMg(CH$_2$Me$_3$) (0.954 mmol) in 5 mL of toluene (alternatively, Mg(CH$_2$CMe$_3$)$_2$(dioxane) may be used as the alkyl source). The purple solution of **1** gradually gave way to a red-orange solution, which was allowed to stir at ambient temperature overnight. The solvent was removed in vacuo, then the residue was dissolved in diethyl ether, filtered, concentrated, and stored at −35 °C. Crystals in the form of yellow needles were collected in the following days. Yield: 28%, 59 mg, 0.089 mmol. MS-CI: [M$^+$] theory 661.3259, experimental 661.3243. ^{1}H NMR (25 °C, C_6D_6): δ 10.97 (s, 1H, C*H*^{t}Bu), 7.20 (s, 2H, Ar*H*), 6.83 (m, 4H, Ar*H*), 2.19 (m (obscured by surrounding peaks), 4H, C*H*Me$_2$), 2.14 (s, 6H, ArC*H$_3$*), 2.1 (1H, C*H*^{t}Bu, located via gHMQC), 1.41 (s, 18H, C*Me$_3$*), 1.16 (d of d, 14H, CH*Me$_2$*), 0.98 (m, 10H, CH*Me$_2$*). ^{1}H NMR (−45 °C, C_7D_8): δ 10.92 (s, 1H, C*H*Me$_3$), 7.23 (m, 1H, Ar*H*), 7.15 (m, 1H, Ar*H*), 6.68 (m, 4H, Ar*H*), 2.13 (s, 3H, ArC*H$_3$*), 2.1 (1H, C*H*Me$_3$, located via-gHMQC), 2.08 (s, 3H, ArC*H$_3$*), 2.05 (m, 2H, C*H*Me$_2$), 1.97 (m, 2H, C*H*Me$_2$), 1.38 (s, 9H, C*Me$_3$*), 1.32 (s, 9H, C*Me$_3$*), 1.08 (m, 12H, CH*Me$_2$*), 0.97 (m, 6H, CH*Me$_2$*), 0.86 (m, 6H, CH*Me$_2$*). ^{31}P NMR (25 °C, C_6D_6): δ 53.9 (broad). ^{31}P NMR (−60 °C, C_7D_8): δ 55.3, 52.2. ^{13}C{^{1}H} NMR (9 °C, 125.69 MHz, C_6D_6): δ 282.5 (Nb=*C*^{t}Bu), 237.1 (Nb=*C*^{t}Bu), 161.5 (*Ar*), 161.3 (*Ar*), 132.7 (*Ar*), 132.4 (*Ar*), 129.0 (*Ar*), 126.3 (*Ar*), 125.1 (*Ar*), 119.9 (*Ar*), 119.2 (*Ar*), 119.1 (*Ar*), 117.2 (*Ar*), 46.3 (*C*Me$_3$), 43.6 (*C*Me$_3$), 35.0 (C*Me$_3$*), 34.0 (C*Me$_3$*), 27.1 (*C*HMe$_2$), 26.5 (*C*HMe$_2$), 25.6 (CH*Me$_2$* or *C*HMe$_2$), 25.1 (CH*Me$_2$* or *C*HMe$_2$), 20.7 (Ar*Me*), 20.4 (CH*Me$_2$* or *C*HMe$_2$), 18.9 (Ar*Me*), 18.6 (CH*Me$_2$* or *C*HMe$_2$), 18.4 (CH*Me$_2$* or *C*HMe$_2$), 18.2 (CH*Me$_2$* or *C*HMe$_2$), 18.1 (CH*Me$_2$* or *C*HMe$_2$), 17.5 (CH*Me$_2$* or *C*HMe$_2$), 16.0 (CH*Me$_2$*), 15.5 (CH*Me$_2$*). One aryl resonance was not located. Multiple attempts to obtain satisfactory combustion analysis were unsuccessful.

Treatment of 3 with $^-$CH$_2$SiMe$_3$. An NMR tube fitted with a J. Young screw-top head was loaded with **3** + **4** (the product mixture containing complexes **3** and **4** in a 3:1 ratio) in C_6D_6. To this solution was added 10 μL of 1,4-dioxane as an internal integration standard. The ^{1}H and ^{31}P NMR spectra of this mixture were recorded. To this solution was added either 1 equiv of LiCH$_2$-SiMe$_3$ or 0.5 equiv of Mg(CH$_2$SiMe$_3$)$_2$. The NMR tube was sealed with a screw-seal Teflon stopper and the solution thoroughly mixed. Monitoring the solution via NMR periodically over the course of 24 h showed no increase in the concentration of **4** relative to 1,4-dioxane, suggesting that **3** is not an intermediate in the synthesis of **4**.

Computational Details. All calculations were carried out using density functional theory as implemented in the Jaguar 6.0 suite[38] of ab initio quantum chemistry programs. Geometry optimizations were performed with the B3LYP[39−42] functional and the 6-31G** basis set with no symmetry restrictions. Niobium was represented using the Los Alamos LACVP basis.[43−45] The energies of the optimized structures were reevaluated by additional single-point calculations on each optimized geometry using Dunning's correlation-consistent triple-ξ basis set[46] cc-pVTZ(-f) that includes a double set of polarization functions. For all transition metals, we used a modified version of LACVP, designated as LACV3P, in which the exponents were decontracted to match the effective core potential with the triple-ξ quality basis. NMR shielding constants are calculated by the method implemented in Jaguar 6.0, with B3LYP and the same basis sets as for the single-point calculation mentioned above. The ^{13}C chemical shifts are calculated as follows:

$$\delta(\text{ppm}) = \sigma(\text{Si}(\text{CH}_3)_4) - \sigma_s$$

$\sigma(\text{Si}(\text{CH}_3)_4)$ is the NMR shielding tensor in Si(CH$_3$)$_4$, and σ_s is the shielding tensor of the atom under investigation.

X-ray Crystallography. General Parameters for Data Collection and Refinement. Single crystals of **3**, **4**, and **5** were grown at room temperature from concentrated solutions of diethyl ether or hexane. Inert-atmosphere techniques were used to place the crystal onto the tip of a glass capillary (0.06−0.20 mm diameter) mounted on a SMART6000 (Bruker) at 113(2) K. A preliminary set of cell constants was calculated from reflections obtained from three nearly orthogonal sets of 20−30 frames. The data collection was carried out using graphite-monochromated Mo Kα radiation with a frame time of 3 s and a detector distance of 5.0 cm. A randomly oriented region of a sphere in reciprocal space was surveyed. Three sections of 606 frames were collected with 0.30° steps in ω at different ϕ settings with the detector set at −43° in 2θ. Final cell constants were calculated from the *xyz* centroids of strong reflections from the actual data collection after integration (SAINT).[47] The structure was solved using SHELXS-97 and refined with SHELXL-97.[48] A direct-methods solution was calculated that provided most non-hydrogen atoms from the E-map. Full-matrix least-squares/difference Fourier cycles were performed that located the remaining non-hydrogen atoms. All non-hydrogen atoms were refined with anisotropic displacement parameters, and all hydrogen atoms were refined with isotropic displacement parameters (unless otherwise specified). Some intensity data were corrected for absorption (SADABS).[49]

Crystallographic details for 3. Inert atmosphere techniques were used to place a black crystal of approximately 0.28 × 0.25 × 0.17 mm onto the tip of a 0.1 mm diameter glass fiber. A total of 76 680 reflections ($-13 \le h \le 13$, $-22 \le k \le 22$, $-30 \le l \le 30$) were collected at $T = 128(2)$ K in the range of 1.90 to 30.03°, of which 8344 were observed ($R_{int} = 0.0482$), Mo Kα radiation ($\lambda = 0.71073$ Å). A direct-methods solution was calculated that provided most non-hydrogen atoms from the E-map. Full-matrix least-squares/difference Fourier cycles were performed, which located the remaining non-hydrogen atoms. The three methyl groups on the Si atom are rotationally disordered over two sites. All non-hydrogen atoms were refined with anisotropic displacement parameters. All hydrogen atoms except those on the disordered methyl groups were located in subsequent Fourier maps and included as isotropic contributors in the final cycles of refinement. Hydrogen atoms on the disordered methyl carbons were placed in ideal positions and refined as riding atoms with relative isotropic displacement parameters. The least-squares refinement converged normally with residuals of $R(F) = 0.0374$, $wR(F^2) = 0.1028$, and a GoF = 1.040 ($I > 2\sigma(I)$). Space group $P2(1)/n$, monoclinic, $a = 9.797(2)$, $b = 16.224(3)$, $c = 21.789(4)$ Å, $\alpha = 90.00°$, $\beta = 101.02(3)°$, $\gamma = 90.00°$, $V = 3399.4(12)$ Å^3, $Z = 4$, $\rho_{calcd} = 1.257$ mg/m^3.

Crystallographic Details for 4. Inert atmosphere techniques were used to place a black crystal of approximate dimensions 0.35 × 0.35 × 0.18 mm onto the tip of a 0.1 mm diameter glass fiber. A total of 120 379 reflections ($-14 \le h \le 14$, $-15 \le k \le 15$, $-40 \le l \le 40$) were collected at $T = 133(2)$ K in the range of 1.85 to 27.55°, of which 13 219 were observed ($R_{int} = 0.0704$), Mo Kα radiation ($\lambda = 0.71073$ Å). A direct-methods solution was calculated, which provided most non-hydrogen atoms from the E-map. Two independent molecules were present in addition to a

(38) *Jaguar*, 5.5 ed.; Schrödinger, L.L.C: Portland, OR, 1991−2003.
(39) Lee, C. T.; Yang, W. T.; Parr, R. G. *Phys. Rev. B* **1988**, *37*, 785.
(40) Becke, A. D. *Phys. Rev. A* **1988**, *38*, 3098.
(41) Becke, A. D. *J. Chem. Phys.* **1993**, *98*, 5648.
(42) Vosko, S. H.; Wilk, L.; Nusair, M. *Can. J. Phys.* **1980**, *58*, 1200.
(43) Hay, P. J.; Wadt, W. R. *J. Chem. Phys.* **1985**, *82*, 270.
(44) Hay, P. J.; Wadt, W. R. *J. Chem. Phys.* **1985**, *82*, 299.
(45) Wadt, W. R.; Hay, P. J. *J. Chem. Phys.* **1985**, *82*, 284.
(46) Dunning, T. H. *J. Chem. Phys.* **1989**, *90*, 1007.
(47) *SAINT*, 6.1 ed.; Bruker Analytical X-ray Systems: Madison, WI, 1999.
(48) *SHELXL-Plus*, 5.10 ed.; Bruker Analytical X-ray Systems: Madison, WI, 1998.
(49) Blessing, R. *Acta Crystallogr.* **1995**, *A51*, 33.

disordered solvent molecule lying near a center of inversion. Full-matrix least-squares/difference Fourier cycles were performed, which located the remaining non-hydrogen atoms. The difference map revealed a disorder in the two $-CH_2SiMe_3$ ligands on both independent molecules. Although most hydrogen atoms were visible in a difference Fourier phased on the non-hydrogen atoms, those associated with the disordered carbon atoms on the ligands were not visible. One-fourth of a disordered Et_2O molecule was confined in the asymmetric unit. The least-squares refinement converged normally with residuals of $R(F) = 0.0357$, $wR(F^2) = 0.09628$, and a GoF = 0.979 ($I > 2\sigma(I)$). $C_{35}H_{62.50}NNbO_{0.25}PSi_2$, space group $P\bar{1}$, triclinic, $a = 11.3020(13)$ Å, $b = 11.7003(13)$ Å, $c = 31.275(4)$ Å, $\alpha = 82.957(3)°$, $\beta = 81.382(3)°$, $\gamma = 77.863(3)°$, $V = 3979.8(8)$ Å^3, $Z = 4$, $\rho_{calcd} = 1.189$ mg/m^3.

Crystallographic Details for 5. Inert atmosphere techniques were used to place a yellow crystal of approximate dimensions 0.13 × 0.13 × 0.11 mm onto the tip of a 0.1 mm diameter glass fiber. A total of 21 572 reflections ($-13 \le h \le 13$, $-14 \le k \le 15$, $-21 \le l \le 21$) was collected at $T = 138(2)$ K in the range of 2.33 to 26.4°, of which 5421 were observed ($R_{int} = 0.0704$), Mo Kα radiation ($\lambda = 0.71073$ Å). A direct methods solution was calculated that provided most non-hydrogen atoms from the E-map. Full-matrix least-squares/difference Fourier cycles were performed, which located the remaining non-hydrogen atoms. A disorder occurs in the two ligands attached to the Nb atom. Because of the disorder, it was not possible to locate the hydrogen atoms associated with the $=CH^tBu$ groups. All non-hydrogen atoms were refined with anisotropic displacement parameters. All hydrogen atoms not associated with the disordered atoms were located in subsequent Fourier maps and included as isotropic contributors in the final cycles of refinement. Hydrogen atoms associated with the disordered atoms were placed in ideal positions and refined as riding atoms with relative isotropic displacement parameters. The least-squares refinement converged normally with residuals of $R(F) = 0.0502$, $wR(F^2) = 0.1137$ and a GoF = 0.905 ($I > 2\sigma(I)$); space group $P\bar{1}$, triclinic, $a = 10.730(4)$ Å, $b = 11.655(4)$ Å, $c = 16.206(6)$ Å, $\alpha = 102.553(9)°$, $\beta = 104.791(9)°$, $\gamma = 103.862(8)°$, $V = 1816.9(12)$ Å^3, $Z = 2$, $\rho_{calcd} = 1.210$ g/cm^3.

Acknowledgment. We thank the Dreyfus Foundation, the Sloan Foundation, and the NSF (CHE-0348941) for financial support of this research. U.J.K. acknowledges the Department of Education for a GAANN Fellowship.

Supporting Information Available: Complete crystallographic data for compounds **3**, **4**, and **5** (CIF) and complete geometrical parameters for the optimized geometries of **4**, **5**, and their computed isomers **A**, **B**, **C**, and **Z** as well as information pertinent to calculation of NMR shifts. This material is available free of charge via the Internet at http://pubs.acs.org.

OM7008233